ISSN 0021-8944, Journal of Applied Mechanics and Technical Physics, 2014, Vol. 55, No. 6, pp. 1045–1054. © Pleiades Publishing, Ltd., 2014.
Original Russian Text © A.A. Ostsemin, P.B. Utkin.

STRESS–STRAIN STATE AND STRESS INTENSITY FACTOR IN THE VICINITY OF CRACK-LIKE DEFECTS UNDER BIAXIAL TENSION OF A PLATE

A. A. Ostsemin[a] **and P. B. Utkin**[b]

UDC 620.170.5; 539.4

Abstract: The problem of determining a stress–strain state described by singular and regular terms and a stress intensity factor in the vicinity of the tip of a crack-like defect in a plate under biaxial loading is considered. The Kolosov–Muskhelishvili method is used to obtain expressions for the stress tensor near the vertex of an ellipse, which yield formulas for stresses in the case of blunt cracks. The maximum shear stress, principal stresses, and stress intensity are determined. Formulas for the stress intensity factor under biaxial loading of a plate with a crack-like defect are obtained and can be used in the holographic interferometry method.

Keywords: fracture mechanics, stress intensity factors, stress state, Kolosov–Muskhelishvili method, plate with an elliptic hole, holographic interferometry method.

DOI: 10.1134/S0021894414060170

INTRODUCTION

One of the reasons for the loss of efficiency of long-distance gas oil pipelines, storage tanks, pressure vessels, torus shells, and a number of other structures is their fracture because of crack-like defects generated in welding and assembly (scratches, guide marks, burrs, and blowholes) or during operation (pitting and corrosive-mechanical cracks) due to metal corrosion. In contrast to cracks, the considered stress concentrators, such as welding defects and corrosive blunted cracks, even the sharpest ones, have a small but finite curvature radius ρ [1].

The methods of fracture mechanics allow one to determine the resistance of metals with cracks to fracture. However, the specific feature of welds is that, even in the absence of cracks, they have stress concentrators with sufficiently small curvature radii, which can be hazardous for operation of such structures. The usage of the fracture mechanics criteria developed to estimate the risk of cracks is incorrect in the case of concentrators (poor penetration, poor fusion, and slag inclusions) typical for welds.

Crack-like defects with a rounded tip cannot be interpreted as sharp cracks, so they cannot be studied by using the criteria of the theory of cracks [2]. The presence of large strain and stress gradients in the vicinity of such concentrators does not allow using the classical strength criteria. The theory of calculation of such defects, which occupies an intermediate position between the theory of cracks and the theory of strength of bodies with structural stress concentrators, has been insufficiently developed [2]. In this paper, we propose a mathematical model of the stress–strain state near the tip of an elliptical defect in a plate under biaxial loading, which takes into account the curvature radius ρ at the tip of the defect.

[a]Russian Presidential Academy of National Economy and Public Administration, Chelyabinsk, 454077 Russia; ostsemin@math.susu.ac.ru. [b]South Ural State University, Chelyabinsk, 454080 Russia; neobart@inbox.ru.
Translated from Prikladnaya Mekhanika i Tekhnicheskaya Fizika, Vol. 55, No. 6, pp. 162–172, November–December, 2014. Original article submitted March 18, 2013; revision submitted December 28, 2013.

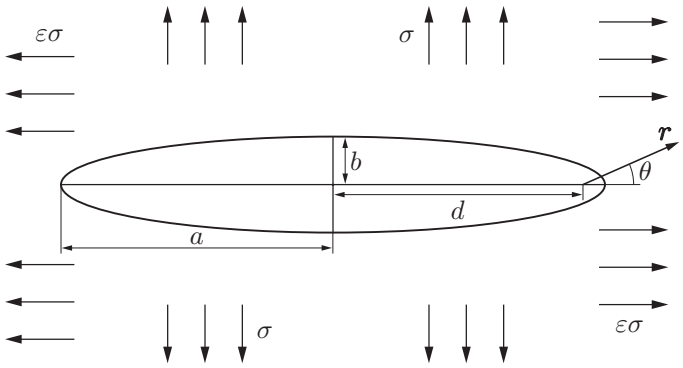

Fig. 1. Diagram of the problem of the elliptical defect in the plate subjected to biaxial loading.

Engineering defects (undercuts, blowholes, cuts, pores, poor penetration, poor fusion, and cracks) impair the resistance of structures to brittle fracture. The radius ρ at the tip of poor penetration can change in a wide range: $\rho = 0.01$–0.10 mm. In this case, the use of the known criteria of linear fracture mechanics, unadjusted for the geometry of crack-like defects and the curvature radius ρ, leads to great errors [2].

Williams [3] obtained a solution to the problem of the elasticity theory for a crack in a plate under uniaxial tension, but the stresses were analyzed only for a singular term.

Eftis et al., mentioned [4] that one should consider the second term in the expansion of the components into a series when solving the problem of determination of the stress and strain tensor components in the case of biaxial loading of a plate with a central crack.

The solution of the problem of the stress distribution around the tip of the cut and the slip line theory were used to develop a model of fracture nucleation [5] at a distance r_c from the tip at a stress σ_c, which was used to derive a formula for the stress intensity factor (SIF) proportional to $\sqrt{\rho}$.

The Kolosov–Muskhelishvili method was used in [6] to obtain approximate formulas for the stress–strain state and the SIF around the tip of an elliptic defect under biaxial loading of a plate [7, 8].

The goals of this work are the approximate calculation of the stress state of a plate near the tip of a crack-like defect with a curvature radius ρ under biaxial loading and the experimental determination of the stress–strain state by the holographic interferometry method.

1. STRESSES AND DISPLACEMENTS IN THE CASE OF A CRACK-LIKE DEFECT OF THE FIRST TYPE UNDER BIAXIAL LOADING OF A PLATE

We consider an engineering crack-like defect in the shape of an elliptic through-hole under biaxial loading of a plate made of an isotropic material.

We assume that an infinite plate with an elliptic hole with semiaxes of lengths a and b is loaded with stresses σ and $\varepsilon\sigma$ along the axes of the initial coordinate system. Figure 1 shows the diagram of this problem (ε is the biaxial loading parameter, i.e., the ratio of the stresses acting in the horizontal and vertical directions). The curvature radius of the elliptical hole in its tip is denoted as $\rho = b^2/a$. The variables r and θ are the coordinates of the polar coordinate system centered at the focus of the ellipse (see Fig. 1).

The values of R and m and the focal length d are the ellipse parameters and are related to the lengths of the ellipse semiaxes a and b by the expressions

$$R = (a+b)/2, \quad m = (a-b)/(a+b), \quad a = R(1+m), \quad b = R(1-m),$$
$$d^2 = a^2 - b^2, \qquad -1 < m < 1, \qquad d^2 = 4ma^2/(1+m)^2 = 4mR^2. \tag{1.1}$$

The distance from the crack tip to the focus of the ellipse is equal to $a - d$ and, at $m \approx 1$, is approximately equal to $\rho/2$. To clarify the relationship between these variables, we can express the ratio $\rho/(2(a-d))$ through the ellipse parameter m. Using Eqs. (1.1), we obtain

$$\frac{\rho}{2(a-d)} = \frac{(1+\sqrt{m})^2}{2(1+m)}. \tag{1.2}$$

Using Eqs. (1.1) and (1.2), we determine the stress tensor components with regular terms near the elliptic through-defect in the plate under biaxial tension:

$$\sigma_x \approx -\frac{DK_{\rm I}}{\sqrt{2\pi r}}\,\frac{\rho}{2r}\cos\Big(\frac{3\theta}{2}\Big) + \frac{A_1K_{\rm I}}{4\sqrt{2\pi r}} - \sigma\Big[\Big(\frac{2r}{\rho}\Big)^{-1/2}D^{3/2}(1+\varepsilon)\cos\Big(\frac{\theta}{2}\Big) - (1-\varepsilon)\,\frac{D^2}{m}\Big]; \tag{1.3}$$

$$\sigma_y \approx \frac{DK_{\rm I}}{\sqrt{2\pi r}}\,\frac{\rho}{2r}\cos\Big(\frac{3\theta}{2}\Big) + \frac{B_1K_{\rm I}}{4\sqrt{2\pi r}} + \sigma\Big[\Big(\frac{2r}{\rho}\Big)^{-1/2}D^{3/2}(1+\varepsilon)\cos\Big(\frac{\theta}{2}\Big) + (1-\varepsilon)\,\frac{D^2-1}{m}\Big]; \tag{1.4}$$

$$\tau_{xy} \approx -\frac{DK_{\rm I}}{\sqrt{2\pi r}}\,\frac{\rho}{2r}\sin\Big(\frac{3\theta}{2}\Big) + \frac{C_1K_{\rm I}}{4\sqrt{2\pi r}} - \sigma\Big(\frac{2r}{\rho}\Big)^{-1/2}D^{3/2}(1+\varepsilon)\sin\Big(\frac{\theta}{2}\Big). \tag{1.5}$$

Here

$$A_1 = \cos(5\theta/2) + (4-2A)\cos(\theta/2), \qquad B_1 = -\cos(5\theta/2) + (2A+4)\cos(\theta/2),$$

$$C_1 = \sin(5\theta/2) - 2A\sin(\theta/2),$$

$$D = (1+m)/(2\sqrt{m}\,), \quad A = (17m^2+6m-15)/(16m), \quad r = |\boldsymbol{r}|.$$

If the ellipse degenerates to a crack ($m = 1$), the first two singular terms in expressions (1.3)–(1.5) correspond to the known formulas [1].

The stress intensity factor is [7]

$$K_{\rm I} = \sqrt[4]{\frac{4m}{(1+m)^2}}\,\sqrt{\pi a}\,\frac{\sigma(m(1+\varepsilon)+(1-\varepsilon))}{2m}, \qquad m = \frac{1-\sqrt{\rho/a}}{1+\sqrt{\rho/a}}. \tag{1.6}$$

It follows from expressions (1.3)–(1.5) that the stress tensor components depend on the parameter of biaxial loading of the plate ε and the nominal tensile stress σ.

The first two terms (singular part) in expression (1.4) are the stress distribution σ_y near the tip of the defect. It follows from expression (1.4) that the two singular terms increase toward the defect tip and begin significantly affecting the stress–strain state. As $r \to 0$, the influence of other terms decreases, whereas the stress field intensity in the vicinity of the defect tip depends only on the SIF value.

Expressions (1.3)–(1.5) for the stress tensor components σ_x, σ_y, and τ_{xy} differ from those given in [1] by the presence of regular terms and a singular term containing $r^{-3/2}$. In the case of a crack ($m = 1$ and $D = 1$), expressions (1.3)–(1.5) correspond to those for the stress components in [4, 7]. For the ellipse parameter $0.9 \leqslant m \leqslant 1.0$, the value of the first principal stress calculated by expressions (1.3)–(1.5) at a distance from the crack tip equal to several tens of the curvature radius ρ differs from the value obtained by the formulas from [1] by not more than 6%.

In view of expressions (1.3) and (1.4), the equation for the sum of the normal stresses $\sigma_x + \sigma_y$ in the case of a central elliptical cutout under biaxial loading of the plate can be written in the following form:

$$\sigma_x + \sigma_y = 2\,\frac{K_{\rm I}}{\sqrt{2\pi r}}\cos\frac{\theta}{2} - \frac{\sigma(1-\varepsilon)}{m}.$$

The equation for the difference of the normal stresses $\sigma_y - \sigma_x$ has the form

$$\sigma_y - \sigma_x = \frac{DK_{\rm I}}{\sqrt{2\pi r}}\,\frac{\rho}{r}\cos\Big(\frac{3\theta}{2}\Big) - \frac{(A_1-B_1)K_{\rm I}}{4\sqrt{2\pi r}}$$

$$+\,\sigma\Big[\Big(\frac{2r}{\rho}\Big)^{-1/2}D^{3/2}(1+\varepsilon)\cos\Big(\frac{\theta}{2}\Big) + (1-\varepsilon)H\Big]. \tag{1.7}$$

Here $H = (1+m^2)/(2m^2)$. In the case of a linear crack, at $\rho = 0$, $m = 1$, and $\theta = 0$, Eq. (1.7) takes the form $\sigma_y - \sigma_x = \sigma(1-\varepsilon) = T$ [4, 5, 9].

In the present problem, the displacements are calculated by the formulas

$$u \approx \frac{1}{2\mu}\Big[\frac{K_{\rm I}}{4}\sqrt{\frac{\rho}{2\pi}}\Big(\frac{r}{\rho}\Big)^{-1/2}\cos\Big(\frac{\theta}{2}\Big) + \frac{\sqrt{r}}{\sqrt{2\pi}}\,D_1 K_{\rm I}$$

$$- \sigma\rho\Big(\frac{r}{\rho}\Big)^{1/2}(1+\varepsilon)\cos\Big(\frac{\theta}{2}\Big) - \frac{\sigma r(1-\varepsilon)}{4}\,(1+\varkappa)\cos\theta - \frac{aT}{4}\,(1+\varkappa)\Big], \tag{1.8}$$

$$v \approx \frac{1}{2\mu}\Big[\frac{K_{\rm I}}{4}\sqrt{\frac{\rho}{2\pi}}\,\Big(\frac{r}{\rho}\Big)^{-1/2}\sin\frac{\theta}{2} + \frac{\sqrt{r}}{\sqrt{2\pi}}\,E_1 K_{\rm I} - \sigma\rho\Big(\frac{r}{\rho}\Big)^{1/2}(1+\varepsilon)\sin\frac{\theta}{2} + \frac{rT}{4}\,(3-\varkappa)\sin\theta\Big],$$

where $D_1 = \cos(\theta/2)(\varkappa - 1 + 2\sin^2(\theta/2))$ and $E_1 = \sin(\theta/2)(\varkappa + 1 - 2\cos^2(\theta/2))$.

At $\rho = 0$, expressions (1.8) yield the well-known formulas given in [4].

2. PRINCIPAL STRESSES IN THE CASE OF A CRACK-LIKE DEFECT UNDER BIAXIAL LOADING OF A PLATE

Considering expressions (1.3)–(1.6), the principal stresses can be calculated by the formula

$$\sigma_{1,2} = \frac{K_{\rm I}}{\sqrt{2\pi r}}\cos\Big(\frac{\theta}{2}\Big) - \frac{\sigma(1-\varepsilon)}{2m} \pm \sqrt{\Big(\frac{K_{\rm I}}{\sqrt{2\pi r}}\Big)^2 F_1 + \frac{2\sigma K_{\rm I}}{\sqrt{2\pi r}}\,F_2 + \sigma^2 F_3}\,, \tag{2.1}$$

where

$$F_1 = D^2\Big(\frac{\rho}{2r}\Big)^2 + D\cos\theta\,\Big(A - \frac{1}{2}\Big)\,\frac{\rho}{2r} + \frac{1}{16}\,(1 - 4A\cos 2\theta + 4A^2),$$

$$F_2 = D^{5/2}\Big(\frac{\rho}{2r}\Big)^{3/2}(1+\varepsilon)\cos\theta + D\,\frac{\rho}{2r}\,(1-\varepsilon)\cos\Big(\frac{3\theta}{2}\Big)\frac{H}{2}$$

$$+ D^{3/2}\Big(\frac{\rho}{2r}\Big)^{1/2}\frac{1+\varepsilon}{4}\,(2A - \cos 2\theta) + \frac{(1-\varepsilon)H}{8}\Big(2A\cos\Big(\frac{\theta}{2}\Big) - \cos\Big(\frac{5\theta}{2}\Big)\Big),$$

$$F_3 = (1+\varepsilon)^2 D^3\,\frac{\rho}{2r} + 2(1-\varepsilon^2)D^{3/2}\Big(\frac{\rho}{2r}\Big)^{1/2}\frac{H}{2}\cos\Big(\frac{\theta}{2}\Big) + (1-\varepsilon)^2\Big(\frac{H}{2}\Big)^2.$$

The distribution of the principal stresses σ_1 and σ_2 calculated by Eq. (2.1) in the case of uniaxial tension of the plate at $\varepsilon = 0$ and $\rho = 0.01$ corresponds to the results obtained in [3]. It is interesting to study the dependences of the principal stresses σ_1 and σ_2 on the polar angle θ by using Eq. (2.1). In the case of uniaxial ($\varepsilon = 0$) tension of the plate, the principal stress σ_1 reaches the greatest value at $\theta = 60^\circ$ and the cut curvature radius values in the range $\rho/a = 0.01$–0.10. In the case of the crack, the maximum value of σ_1 is also reached at $\theta = 60^\circ$ [3].

The stress intensity σ_i calculated according to the von Mises plasticity criterion in the case of a plane stress state in the plate with a central elliptical cutout in view of expressions (1.3)–(1.5) is equal to

$$\sigma_i^2 = \Big(\frac{K_{\rm I}}{\sqrt{2\pi r}}\Big)^2\Big(\cos^2\Big(\frac{\theta}{2}\Big) + 3F_1\Big) + \frac{2\sigma K_{\rm I}}{\sqrt{2\pi r}}\Big[-\frac{1-\varepsilon}{2m}\Big(\cos\Big(\frac{\theta}{2}\Big)$$

$$+ 3\,\frac{1+m^2}{4m}\Big(\frac{1}{2}\cos\Big(\frac{5\theta}{2}\Big) - A\cos\Big(\frac{\theta}{2}\Big)\Big)\Big) - \frac{3(1+\varepsilon)}{4}\,D^{1/2}\Big(\frac{\rho}{2r}\Big)^{1/2}\Big(\cos 2\theta - 2A\Big)$$

$$+ \frac{3(1-\varepsilon)}{4m^2}\,D\,\frac{\rho}{2r}\cos\Big(\frac{3\theta}{2}\Big) + 3(1+\varepsilon)D^{5/2}\Big(\frac{\rho}{2r}\Big)^{3/2}\cos\theta\Big]$$

$$+ \sigma^2\Big[\Big(\frac{1-\varepsilon}{m}\Big)^2 + 3(1-\varepsilon)^2\Big(\frac{1-m^2}{4m^2}\Big)^2 + 3(1+\varepsilon)^2 D^3\,\frac{\rho}{2r} + 3(1-\varepsilon^2)D^{3/2}\Big(\frac{\rho}{2r}\Big)^{1/2}\cos\Big(\frac{\theta}{2}\Big)H\Big]. \tag{2.2}$$

At $\sigma_i = \sigma_{\rm yield}$ ($\sigma_{\rm yield}$ is the yield point), we can use Eq. (2.2) to determine the size of the plastic zone in the cut in the same way as it was done in [5].

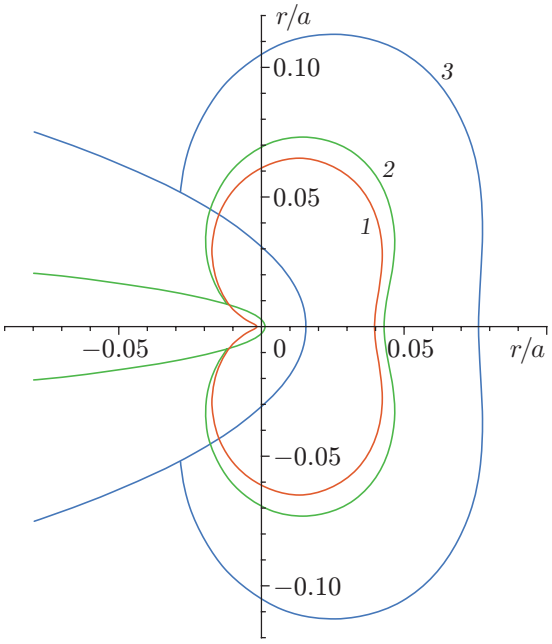

Fig. 2. Shapes of the plastic zone for different values of the ellipse parameter: $m = 1$ (*1*), 0.9 (*2*), and 0.7 (*3*).

To construct the lines of constant intensity levels for the stresses σ_i under biaxial loading of the plate, numerical methods should be used because the quantity $\sqrt{r}$ in Eq. (2.2) has a sixth power. Figure 2 shows the plastic zone radius in the case of tension of the plate with an elliptical cutout at $\sigma = 0.3\sigma_{\text{yield}}$ and $\varepsilon = 0.5$. A decrease in the parameter of biaxial loading of the plate $\varepsilon = 0.5$ to $\varepsilon = 0$ significantly increases the area of the plastic zone. As the nominal stress σ_{nom} becomes larger, the area of the plastic zone in the case of uniaxial tension ($\varepsilon = 0$) increases faster than in the case of biaxial loading ($\varepsilon = 0.5$).

Earlier, the radius of the plastic zone at the defect tip was estimated by using the formula for the stress in the vicinity of the crack. The obtained approximate formulas along with the von Mises criterion allow us to estimate the sizes of the plastic zones near the tip of the defect with an elliptical contour. The plastic zone radii calculated by the formulas for the crack and the ellipse with the parameter $m = 0.9$ have different values in different directions. In the case of the central elliptic defect, the difference in the radii ranges from 7 to 20%, wherein the smallest difference occurs on the axis of the defect.

3. MAXIMUM SHEAR STRESS IN THE CASE OF A CRACK-LIKE DEFECT UNDER BIAXIAL LOADING OF A PLATE

Using expressions (1.3)–(1.7), we write the formula for the maximum shear stress $\tau_{\max}$ near the tip of the elliptical defect:

$$\tau_{\max}^2 = \Big(\frac{K_{\text{I}}}{\sqrt{2\pi r}}\Big)^2 F_1 + \frac{\sigma K_{\text{I}}}{\sqrt{2\pi r}} F_2 + \sigma^2 F_3. \tag{3.1}$$

It follows from Eq. (3.1) that the positions on the line level $\tau_{\max}$ depends on the biaxial loading parameter ε, cut curvature radius ρ, and stress σ.

In the case of a straight-line crack ($m = 1$), formula (3.1) for $\tau_{\max}$ corresponds to the theoretical results [4] and is used to determine K_{I} from isochrome patterns by the photoelasticity method.

Figure 3 shows the dependence of the ratio of the maximum shear stress for a plate with an elliptic cutout at $\theta = 0$ to the maximum shear stress for a crack at the same defect length (the crack length is equal to the length of the major axis of the ellipse: $2l = 2a$) at a distance from the crack tip equal to $0.07a$ on the ellipse parameter m.

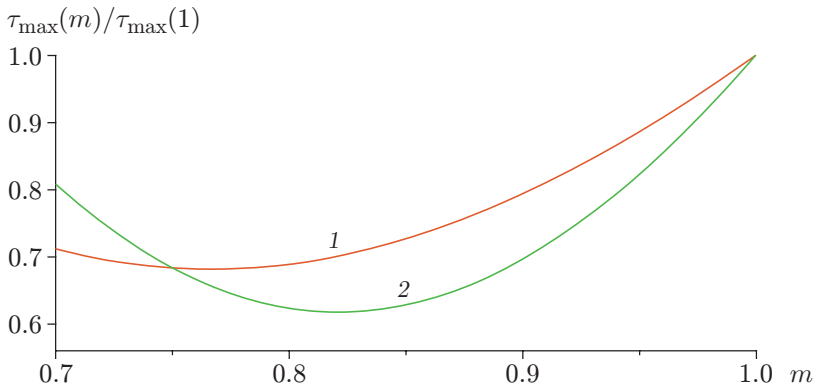

Fig. 3. Maximum shear stresses versus the ellipse parameter m for $\varepsilon = 0$ (*1*) and 0.5 (*2*).

4. STRESS TENSOR COMPONENTS IN THE POLAR COORDINATES FOR A DEFECT OF THE FIRST TYPE UNDER BIAXIAL LOADING OF A PLATE

The stress tensor components in the polar coordinates can be found by transforming expressions (1.3)–(1.5) for the stresses σ_x, σ_y, and τ_{xy}. After a series of transformations, we write the expressions for the stress tensor components with regular terms in the case of the elliptic defect in the polar coordinates as functions of the cut curvature radius ρ and the parameter of biaxial loading of the plate ε:

$$\sigma_r \approx -\frac{DK_{\mathrm{I}}}{\sqrt{2\pi r}}\,\frac{\rho}{2r}\cos\Big(\frac{\theta}{2}\Big) + \frac{K_{\mathrm{I}}}{4\sqrt{2\pi r}}\Big(5\cos\Big(\frac{\theta}{2}\Big) - \frac{17m^2+6m-15}{8m}\cos\Big(\frac{3\theta}{2}\Big)\Big)$$

$$-\Big(\frac{2r}{\rho}\Big)^{-1/2} D^{3/2}\sigma(1+\varepsilon)\cos\Big(\frac{3\theta}{2}\Big) - T\Big(\Big(\frac{1+m}{2m}\Big)^2\cos^2\theta - \Big(\frac{1-m}{2m}\Big)^2\sin^2\theta\Big); \tag{4.1}$$

$$\sigma_\theta \approx \frac{DK_{\mathrm{I}}}{\sqrt{2\pi r}}\,\frac{\rho}{2r}\cos\Big(\frac{\theta}{2}\Big) + \frac{K_{\mathrm{I}}}{4\sqrt{2\pi r}}\Big(3\cos\Big(\frac{\theta}{2}\Big) + \frac{17m^2+6m-15}{8m}\cos\Big(\frac{3\theta}{2}\Big)\Big)$$

$$+\Big(\frac{2r}{\rho}\Big)^{-1/2} D^{3/2}\sigma(1+\varepsilon)\cos\Big(\frac{3\theta}{2}\Big) - T\Big(\Big(\frac{1+m}{2m}\Big)^2\sin^2\theta - \Big(\frac{1-m}{2m}\Big)^2\cos^2\theta\Big),$$

$$\tau_{r\theta} \approx \frac{DK_{\mathrm{I}}}{\sqrt{2\pi r}}\,\frac{\rho}{2r}\sin\Big(\frac{\theta}{2}\Big) + \frac{K_{\mathrm{I}}}{4\sqrt{2\pi r}}\Big(\sin\Big(\frac{\theta}{2}\Big) + \frac{17m^2+6m-15}{8m}\sin\Big(\frac{3\theta}{2}\Big)\Big) - \Big(\frac{2r}{\rho}\Big)^{-1/2} D^{3/2}\sigma(1+\varepsilon)\sin\Big(\frac{3\theta}{2}\Big) + TH\sin 2\theta.$$

5. STRAIN STATE AT THE TIP OF A CRACK-LIKE CUT UNDER BIAXIAL LOADING OF A PLATE

The elastic strains in the cut region are determined by using formulas (1.3)–(1.4) for the case of a plane stress state ($\sigma_z = 0$) based on Hooke's law:

$$\varepsilon_x = \frac{1}{E}\Big(-\frac{K_{\mathrm{I}}D(1+\mu)}{\sqrt{2\pi r}}\,\frac{\rho}{2r}\cos\Big(\frac{3\theta}{2}\Big) + \frac{K_{\mathrm{I}}}{4\sqrt{2\pi r}}\,(A_1 - \mu B_1)$$

$$-(1+\mu)\Big(\frac{2r}{\rho}\Big)^{-1/2} D^{3/2}\sigma(1+\varepsilon)\cos\Big(\frac{\theta}{2}\Big) - \sigma(1-\varepsilon)\Big(\Big(\frac{1+m}{2m}\Big)^2 + \mu\Big(\frac{1-m}{2m}\Big)^2\Big)\Big),$$

$$\varepsilon_y = \frac{1}{E}\Big(\frac{D(1+\mu)}{\sqrt{2\pi r}}\,\frac{\rho}{2r}\,K_{\rm I}\cos\Big(\frac{3\theta}{2}\Big) + \frac{K_{\rm I}}{4\sqrt{2\pi r}}\,(B_1 - \mu A_1)$$
$$+ (1+\mu)\Big(\frac{2r}{\rho}\Big)^{-1/2} D^{3/2}\sigma(1+\varepsilon)\cos\Big(\frac{\theta}{2}\Big) + \sigma(1-\varepsilon)\Big(\Big(\frac{1-m}{2m}\Big)^2 + \mu\Big(\frac{1+m}{2m}\Big)^2\Big)\Big),$$
$$\varepsilon_z = \frac{2\mu}{E}\Big(\frac{K_{\rm I}}{\sqrt{2\pi r}}\cos\Big(\frac{\theta}{2}\Big) - \frac{\sigma(1-\varepsilon)}{2m}\Big), \qquad \gamma_{xy} = \frac{\tau_{xy}}{G}.$$

Here $G = E/(2(1+\mu))$ is the shear modulus, E is Young's modulus, and μ is Poisson's ratio.

6. DETERMINATION OF THE STRESS INTENSITY FACTOR FOR A CRACK-LIKE DEFECT BY THE HOLOGRAPHIC INTERFEROMETRY METHOD

Doyle et al. [10] determined the effect of the curvature radius ρ at the cut tip and analyzed the errors in the calculation of $K_{\rm I}$ in the plate on the basis of the formulas obtained in [1]. Etheridge and Dalley [9] overviewed the Irvine, Bradley–Kobayashi, and Smith methods of using the two-parameter photoelasticity to determine the experimental values of $K_{\rm I}$ under biaxial loading of the plate with a central crack on the basis of isochrome patterns. The holographic interferometry method was used in [11] to study the stress state, the formulas [1] were used to calculate the stress intensity factor $K_{\rm I}$ in a plate with a crack-like defect, and the experiment was described. In accordance with von Neumann's theory and Hooke's law, assuming that strains are small, we have a relationship for thin plates between the numbers of interference fringes on the patterns of absolute path differences (APDs) and the principal stresses σ_1 and σ_2 in the form of Favre's relations [12]:

$$N_1 = a\sigma_1 + b\sigma_2, \qquad N_2 = b\sigma_1 + a\sigma_2, \tag{6.1}$$

where N_1 are N_2 are the fringe numbers in the APD patterns with vertical and horizontal polarizations of the reference beam, respectively; $a = 0.625$ fringes/MPa and $b = 0.453$ fringes/MPa are the optical constants of the ED-20MPGFA material. For an elastic material, Ostsemin et al. [13] described a calibration method providing high accuracy of determining the constants a and b by using all the observed interference fringes and applying interpolation operations for determining the fringe numbers. The APD patterns may be conveniently processed along the axis of the crack-like defect at $\theta = 0$ (the largest number of interference fringes). In the case of $\sigma_1 = \sigma_y$, $\sigma_2 = \sigma_x$, and $\tau_{xy} = 0$, Eq. (2.1) yields:

$$\sigma_{1,2} = \frac{K_{\rm I}}{\sqrt{2\pi r_i}}\Big(1 \pm \Big(D\,\frac{\rho}{2r_i} + \frac{2A-1}{4}\Big)\Big) - \sigma\Big(\frac{1-\varepsilon}{2m} \mp \Big((1+\varepsilon)D^{3/2}\Big(\frac{\rho}{2r_i}\Big)^{1/2} + (1-\varepsilon)\,\frac{H}{2}\Big)\Big). \tag{6.2}$$

The difference of experimental and theoretical values of σ_1 is about 6%.

Earlier, calculations were performed by using the formula for the SIF for cracks. In this paper, we obtained formulas for the SIF for an elliptic cutout in a plate, which generalize the formulas for cracks. At $m = 0.97$, the difference of the present SIF values from the SIF calculated for the case of a linear cut (crack) is more than 10%.

Substituting Eq. (6.2) in Eqs. (6.1), we obtain formulas for the interference fringes with the numbers N_{1i}:

$$N_{1i} = \frac{K_{\rm I}}{\sqrt{2\pi r_i}}\,((a+b) + (a-b)B) - \sigma\Big(\frac{(1-\varepsilon)(a+b)}{2m} - (a-b)C\Big). \tag{6.3}$$

Here

$$B = D\,\frac{\rho}{2r_i} + \frac{17m^2 - 2m - 15}{32m}, \quad C = (1+\varepsilon)D^{3/2}\Big(\frac{\rho}{2r_i}\Big)^{1/2} + (1-\varepsilon)\,\frac{H}{2}.$$

From Eq. (6.3), we have

$$K_{{\rm I}i} = \sqrt{2\pi r_i}\,\frac{N_{1i} + \sigma((1-\varepsilon)(a+b)/(2m) - (a-b)C)}{(a+b) + (a-b)B}. \tag{6.4}$$

Using the results obtained and formula (6.4), we calculate the value of $K_{\rm I}^{\rm exp} = 25.89$ MPa$\cdot$mm$^{1/2}$, which agrees with the calculated value $K_{\rm I}^{\rm calc} = 24.88$ MPa$\cdot$mm$^{1/2}$ with a 4% error. It is known that the SIF value in the case of tension of a finite-size plate with a central crack-like defect is [2, 5]

$$K_{\rm I} = \sigma_{\rm nom}\sqrt{\pi l}\,f_1. \tag{6.5}$$

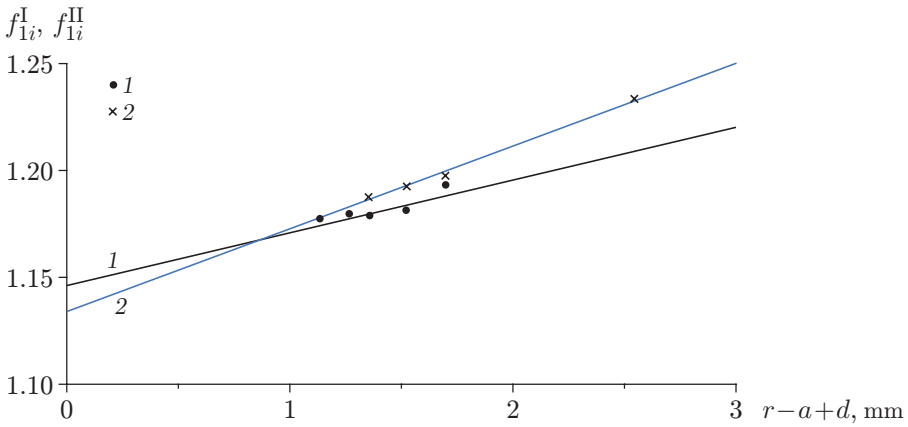

Fig. 4. Extrapolation of the experimental values of f_{1i}^{I} (*1*) and f_{1i}^{II} (*2*).

Here l is the half-length of the defect and f_1 is the correction function depending on the sample geometry and the loading type.

Equating the right sides of Eqs. (6.4) and (6.5) and taking into account that $\sigma = \sigma_{\mathrm{nom}}$, we obtain expressions for the correction function f_{1i} depending on N_{1i} and N_{2i}:

$$f_{1i}^{\mathrm{I}} = \sqrt{\frac{2r_i}{l}}\,\frac{N_{1i} + \sigma_{\mathrm{nom}}((1-\varepsilon)(a+b)/(2m) - (a-b)C)}{\sigma_{\mathrm{nom}}((a+b) + (a-b)B)}; \tag{6.6}$$

$$f_{1i}^{\mathrm{II}} = \sqrt{\frac{2r_i}{l}}\,\frac{N_{2i} + \sigma_{\mathrm{nom}}((1-\varepsilon)(a+b)/(2m) + (a-b)C)}{\sigma_{\mathrm{nom}}((a+b) - (a-b)B)}. \tag{6.7}$$

Validation of Eqs. (1.4) for σ_y, (6.4) for the SIF K_{I}, (6.6) for the correction function f_{1i}^{I}, and (6.7) for f_{1i}^{II} was performed by the holographic interferometry method [11]. The experiments were carried out for a plate 100 mm in width and 3.83 mm in thickness with a central elliptic hole of length of 30 mm and radius $\rho = 0.15$ mm, which was subjected to uniaxial loading ($\varepsilon = 0$) under the nominal stress $\sigma_{\mathrm{nom}} = 3.28$ MPa.

Using the patterns of N_{1i} with formula (6.6) in the case of vertical polarization of the reference beam and the patterns of N_{2i} with formula (6.7) in the case of horizontal polarization of the reference beam, we find the values of the correction functions f_{1i}^{I} and f_{1i}^{II}. The values of f_{1i}^{I} and f_{1i}^{II} in Fig. 4 are extrapolated by straight lines.

The experimentally obtained values $f_1^{\mathrm{I}} = 1.15$ and $f_1^{\mathrm{II}} = 1.14$ are greater than $f_1 = 1.06$ obtained by the Feddersen formula [5]. This is due to the presence of regular terms in formulas (6.6) and (6.7) because of accounting for the second term in the Williams representation [3] of the stress tensor components [4, 5, 7].

We obtain approximate formulas for the stress tensor, which take into account the curvature of the defect as well as singular and regular terms of expansion, while previously only singular terms were accounted for. When estimating the maximum principal stress at the defect tip significantly affecting the fracture criteria, the difference of the values obtained by the formulas for the crack and the ellipse is over 50%. At a distance from the defect tip, equal to 10 curvature radii, the above-mentioned difference along the major axis of the defect is greater than 10%.

If regular terms are omitted in the formulas for the stresses, there may be errors in the calculation of structures with crack-like defects and their brittle fracture.

Formula (6.1) for the principal stresses σ_1 and σ_2 is used to obtain a formula for determining the stress intensity σ_i from APD patterns [13]:

$$\sigma_i^2 = \frac{(a^2+ab+b^2)N_1^2 - (a^2-4ab+b^2)N_1N_2 + (a^2+ab+b^2)N_2^2}{(a^2-b^2)^2}. \tag{6.8}$$

Figure 5 shows the dependences of the stress intensity σ_i on the distance r, which were calculated by formula (6.8) (points) and formula (2.2) (curve). The difference of the values obtained is 10%.

Figure 6 shows the dependences of the difference between the principal stress intensities $\sigma_1 - \sigma_2$ on the distance r calculated by formula (1.7) (curve) and relations (4.1) (points).

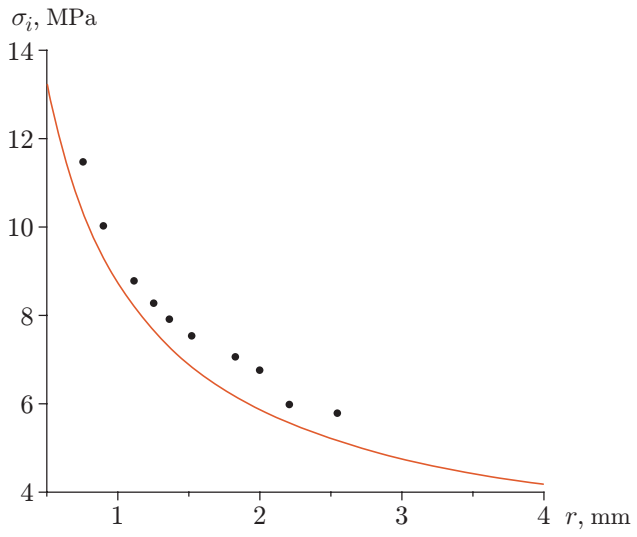

Fig. 5.

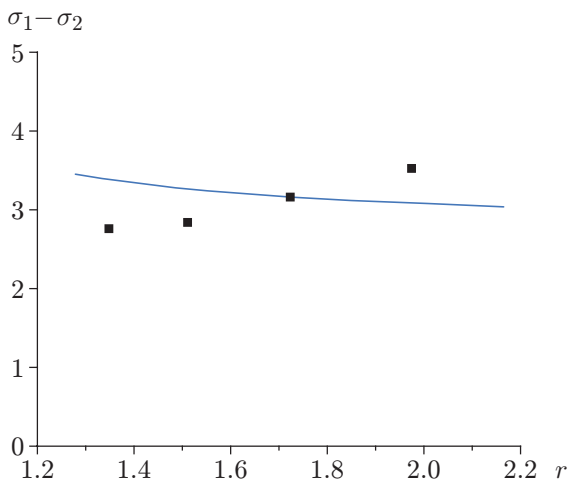

Fig. 6.

Fig. 5. Experimental (points) and theoretical (curve) dependences of the stress intensity σ_i on the distance from the defect tip.

Fig. 6. Experimental (points) and theoretical (curve) dependences of the difference between the principal stresses $\sigma_1 - \sigma_2$ on the distance from the defect tip.

The results of the theoretical studies performed in this paper agree with the experimental data [14] for ferrite–pearlite steels and using the model of brittle fracture [15].

Ostsemin and Utkin [16] used exact formulas to study the effect of regular terms on the stress–strain state (σ_1, σ_i, and SIF) under biaxial loading of a plate with an inclined elliptic cutout.

CONCLUSIONS

In this paper, the formulas for the stress tensor components, the principal stresses, the stress intensity, the maximum shear stress, and the sum and difference of the principal stresses with regular terms for a crack-like defect with a curvature radius ρ under biaxial tension of a plate were obtained.

The holographic interferometry method was used to obtain the experimental values of the stress intensity σ_i and the stress difference $\sigma_y - \sigma_x$ as well as the coefficients for the correction functions used to calculate the SIF.

In the case of a central elliptical hole with a curvature radius $\rho = 0.15$ mm, the experimental values of σ_1, σ_i, and K_{I} determined by the holographic interferometry method agree with the calculated values with an error of 6, 10, and 4%, respectively.

REFERENCES

1. M. Creager and P. Paris, "Elastic Field Equations for Blunt Cracks with Reference to Stress Corrosion Cracking," Int. J. Fracture Mech. **4** (3), 247–252 (1967).
2. V. B. Panasyuk, *Quasibrittle Fracture Mechanics* (Naukova Dumka, Kiev, 1991) [in Russian].
3. M. L. Williams, "On the Stress Distribution at the Base of a Stationary Crack," J. Appl. Mech. **24** (1), 109–114 (1957).
4. J. Eftis, N. Subramonian, and H. Liebowitz, "Crack Border Stress and Displacement Equations Revisited," Eng. Fracture Mech. **9** (1), 189–210 (1977).
5. A. Ya. Krasovskii, *Brittleness of Metals at Low Temperatures* (Naukova Dumka, Kiev, 1980).
6. N. I. Muskhelishvili, *Some Basic Problems of the Mathematical Theory of Elasticity* (Nauka, Moscow, 1966).

7. A. A. Ostsemin and P. B. Utkin, "Theoretical and Experimental Research on the Fracture Mechanics of Crack-Like Defects under Biaxial Loading," Izv. Ross. Akad. Nauk, Mekh. Tverd. Tela, No. 2, 130–142 (2009).
8. A. A. Ostsemin and P. B. Utkin, "Application of the Criteria of Elastoplastic Fracture Mechanics for Estimating the Properties of Welded Joints," Vopr. Materialoved., No. 3, 151–160 (2007).
9. J. M. Etheridge and J. W. Dalley, "A Critical Review of Methods for Determining Stress-Intensity Factors from Isochromatic Fringes," Exp. Mech. **17** (7), 248–254 (1977).
10. J. F. Doyle, S. Kamle, and J. Takezaku, "Error Analysis of Photoelasticity in Fracture Mechanics," Exp. Mech. **21** (11), 429–435 (1981).
11. A. A. Ostsemin, "Determination of the Stress State and the Stress Intensity Factors of Crack-Like Defects by Holographic Interferometry," Vest. Mashinostr., No. 8, 13–19 (2009).
12. A. Ya. Aleksandrov and M. Kh. Akhmetzyanov, *Polarization-Optical Methods of Deformable Solid Mechanics* (Nauka, Moscow, 1973) [in Russian].
13. A. A. Ostsemin, S. A. Deniskin, L. L. Sitnikov, et al., "Determining the Stress State of Bodies with Defects by Using Holographic Photoelasticity," Probl. Prochn., No. 10, 77–81 (1982).
14. J. Malkin and A. S. Tetelman, "Relation between $K_{\mathrm{I}c}$ and Microscopic Strength for Low Alloy Steels," Eng. Fracture Mech. **3** (2), 151–167 (1971).
15. R. O. Ritche, G. F. Knott, and J. R. Rice, "On the Relation Between Critical Tensile Stress and Fracture Toughness in Mild Steel," J. Mech. Phys. Solids **21** (6), 395–410 (1973).
16. A. A. Ostsemin and P. B. Utkin, "Stress–Strain State of an Inclined Elliptical Defect in a Plate Under Biaxial Loading," Prikl. Mekh. Tekh. Fiz. **53** (2), 115–127 (2012) [J. Appl. Mech. Tech. Phys. **53** (2), 246–257 (2012)].